

Higgs searches and singlet scalar dark matter: Combined constraints from XENON 100 and the LHC

Yann Mambrini^{1,*}

¹*Laboratoire de Physique Théorique, Université Paris-Sud, F-91405 Orsay, France*
(Received 5 October 2011; published 23 December 2011)

XENON100 and the LHC are two of the most promising machines to test the physics beyond the standard model. In the meantime, indirect hints push us to believe that the dark matter and Higgs boson could be the two next fundamental particles to be discovered. Whereas ATLAS and CMS have just released their new limits on the Higgs searches, XENON100 obtained very recently strong constraints on dark matter–proton elastic scattering. In this work, we show that when we combined WMAP and the most recent results of XENON100, the invisible width of the Higgs to scalar dark matter is negligible ($\leq 10\%$), except in a small region with very light dark matter (≤ 10 GeV) not yet excluded by XENON100 or around 60 GeV where the ratio can reach 50% to 60%. The new results released by the Higgs searches of ATLAS and CMS set very strong limits on the elastic scattering cross section, even restricting it to the region $8 \times 10^{-46} \text{ cm}^2 \leq \sigma_{S-p}^{\text{SI}} \leq 2 \times 10^{-45} \text{ cm}^2$ in the hypothesis $135 \text{ GeV} \leq M_H \leq 155 \text{ GeV}$.

DOI: [10.1103/PhysRevD.84.115017](https://doi.org/10.1103/PhysRevD.84.115017)

PACS numbers: 95.35.+d, 12.60.Cn, 14.80.Da

I. INTRODUCTION

Two of the most important issues in particle physics phenomenology are the nature of dark matter and the mechanism to realize spontaneously the electroweak symmetry breaking of the standard model (SM). The observations made by the WMAP Collaboration [1] show that the matter content of the Universe is dark, making up about 85% of the total amount of matter, whereas the XENON Collaboration recently released its constraints on direct detection of dark matter [2]. These constraints are the most stringent in the field nowadays, and begin to exclude a significant part of the parameter space of the weakly interacting massive particle (WIMP) paradigm. In the meantime, the accelerator collaborations ATLAS [3], CMS [4], and D0/CDF [5,6] presented their results concerning the Higgs searches. It is obvious that the Higgs hunting at the LHC is intimately linked with measurement of elastic scattering on the nucleon, especially in Higgs-portal-like models where the Higgs boson is the key particle exchanged through annihilation/scattering processes. It has already been showed recently that a combined LEP/TEVATRON/XENON/WMAP analysis can severely restrict the parameter space allowed in generic constructions [7]. In this work, we apply such an analysis in the specific context of a scalar singlet dark matter extension of the standard model and show that most of the region allowed by WMAP will be excluded/probed by the LHC and XENON100 by the end of next year.

The paper is organized as follows: we summarize in Sec. II the scalar singlet extension of the standard model and study its direct detection modes based on recent analysis of the nucleon structure and their influences on the detection prospects. We then devote Sec. III to the invisible

branching ratio of the Higgs. We show that after combining WMAP and the last XENON100 constraints, the invisible width of the Higgs is negligible, making it a SM Higgs for which ATLAS and CMS observability studies can be applied. We then include in Sec. IV the new LHC/TEVATRON analyses released very recently and show that a large part of the parameter space of the model is already excluded. We then concentrate in Sec. V on the direct detection cross section one can expect if a Higgs boson mass $M_H \approx 145$ GeV is observed in the near future. We then conclude in Sec. VI.

II. DIRECT DETECTION AND NUCLEON STRUCTURE

A. The model

The simplest extension of the SM is the addition of a real singlet scalar field. Although it is possible to generalize to scenarios with more than one singlet, the simplest case of a single additional singlet scalar provides a useful framework to analyze the generic implications of an augmented scalar sector to the SM. The most general renormalizable potential involving the SM Higgs doublet H and the singlet S is

$$\begin{aligned} \mathcal{L} = & \mathcal{L}_{\text{SM}} + (D_\mu H)^\dagger (D^\mu H) + \frac{1}{2} \mu_H^2 H^\dagger H - \frac{1}{4} \lambda_H H^4 \\ & + \frac{1}{2} \partial_\mu S \partial^\mu S - \frac{\lambda_S}{4} S^4 - \frac{\mu_S^2}{2} S^2 - \frac{\lambda_{HS}}{4} S^2 H^\dagger H \\ & - \frac{\kappa_1}{2} H^\dagger H S - \frac{\kappa_3}{3} S^3 - V_0, \end{aligned} \quad (1)$$

where D_μ represents the covariant derivative. We have eliminated a possible linear term in S by a constant shift, absorbing the resulting S -independent term in the vacuum energy V_0 . We require that the minimum of the potential

*Yann. Mambrini@th.u-psud.fr

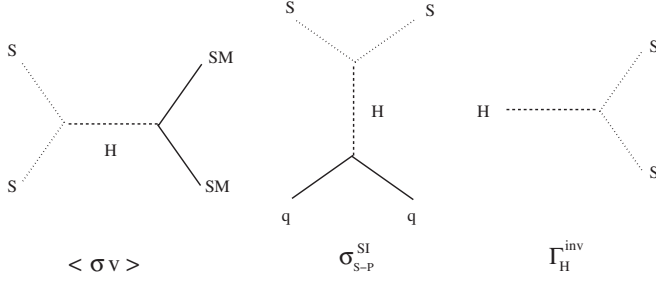


FIG. 1. Feynman diagram for the annihilation cross section (left), direct detection scattering (center), and invisible width of the Higgs (right).

occur at $v = 246$ GeV. Fluctuations around this vacuum expectation value are the SM Higgs boson. For the case of interest here for which S is stable and may be a dark matter candidate, we impose a Z_2 symmetry on the model, thereby eliminating the κ_1 and κ_3 terms. We also require that the true vacuum of the theory satisfies $\langle S \rangle = 0$, thereby precluding mixing of S and the SM Higgs boson and the existence of cosmologically problematic domain walls. In this case, the masses of the scalars are

$$M_H = \sqrt{2}\mu_H, \quad m_S = \sqrt{\mu_S^2 + \frac{\lambda_{HS}}{\lambda_H} \frac{\mu_H^2}{2}}, \quad (2)$$

and the HSS coupling generated is

$$C_{HSS}: -\frac{\lambda_{HS}M_W}{2g}. \quad (3)$$

We show in Fig. 1 the Feynman diagrams relevant for our analysis.¹ Different aspects of the scalar singlet extension of the SM have already been studied in [8–22], whereas a nice preliminary analysis of its dark matter consequences can be found in [23]. Some authors also tried to explain the DAMA and/or COGENT excess [24–26], whereas other authors probed the model by indirect searches [27–29], or looked at the consequences of earlier XENON data [30–32].

B. The nucleon structure uncertainties

For several years it has been known that the uncertainties generated by the quark contents of the nucleons can be as important (if not more) than astrophysical uncertainties. Some authors pointed out this issue and applied it to supersymmetric models [33,34], in an effective operator approach [35] or even in the scalar extension of the SM [24], but rarely taking into account the latest lattice results [34]. Indeed, due to its large Yukawa coupling, the strange quark and its

¹The quartic coupling $SSHH$ which can be efficient in the computation of the relic abundance if $m_s \gtrsim M_H$ is also present. We obviously took it into account in our numerical analysis but its contribution to the annihilation processes is always subdominant.

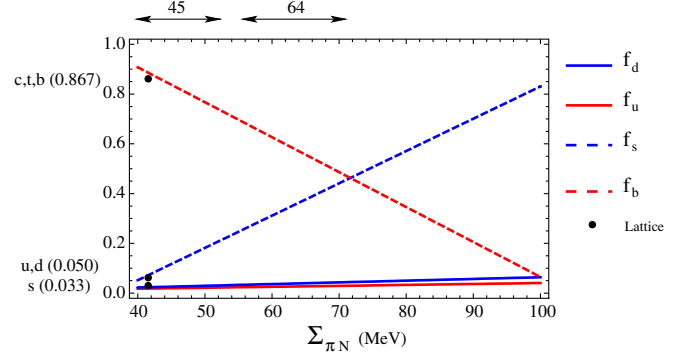


FIG. 2 (color online). Sigma commutators of the proton with two different phenomenological measurements of $\Sigma_{\pi N} = 45 \pm 8$ MeV [39] and 64 ± 7 MeV [40]. We also show the mean evaluation from more recent lattice results [43] (left).

content in the nucleon are of particular interest in the elastic scattering of the dark matter on the proton. The spin-independent part of the cross section can be written

$$\sigma_{S-N}^{SI} = \frac{4m_r^2}{\pi} [Zf_p + (A - Z)f_n]^2, \quad (4)$$

where $m_r = m_N m_S / (m_S + m_N)$ is the S -nuclear reduced mass and

$$f_N = m_N \left(\sum_{q=u,d,s} f_q^N \frac{\mathcal{A}_q}{m_q} + \frac{2}{27} f_H^N \sum_{q=c,b,t} \frac{\mathcal{A}_q}{m_q} \right) \quad (5)$$

with \mathcal{A}_q the scattering amplitude on a single quark q , and $f_q^N = (m_q/m_N) \langle N | \bar{q}q | N \rangle$ is the reduced (dimensionless) sigma terms of the nucleon N , and $f_H^N = 1 - \sum_{q=u,d,s} f_q^N$ [36,37].

There are different ways of extracting the reduced dimensionless nucleon (N) sigma terms $f_q^N \equiv (m_q/m_N) \langle N | \bar{q}q | N \rangle$. These sigma terms can be derived by phenomenological estimates of the $\pi - N$ scattering $\Sigma_{\pi N}$ (see [38] and references therein for a review): $\Sigma_{\pi N} \equiv m_l f_l = m_l \langle N | \bar{u}u + \bar{d}d | N \rangle$ with $m_l = (m_u + m_d)/2$. While an early experimental extraction [39] gave $\Sigma_{\pi N} = 45 \pm 8$ MeV, a more recent determination [40] obtained $\Sigma_{\pi N} = 64 \pm 7$ MeV.

On the other hand, the study of the breaking of $SU(3)$ within the baryon octet and the observation of the spectrum lead to deriving a constraint on the nonsinglet combination $\sigma_0 = m_l \langle N | \bar{u}u + \bar{d}d - 2\bar{s}s | N \rangle$. Chiral effective field theory leads to a value $\sigma_0 = 36 \pm 7$ MeV. Following [41] by introducing $z = (\langle N | \bar{u}u + \bar{s}s | N \rangle) / (\langle N | \bar{d}d + \bar{s}s | N \rangle) = 1.49$ one obtains

$$\begin{aligned} f_d &= \frac{m_d}{m_N} \frac{\Sigma_{\pi N}}{m_u + m_d} \frac{y(z-1) + 2}{1+z}, \\ f_u &= \frac{m_u}{m_N} \frac{\Sigma_{\pi N}}{m_u + m_d} \frac{y(1-z) + 2z}{1+z}, \\ f_s &= \frac{m_s}{m_N} \frac{\Sigma_{\pi N}}{m_u + m_d} y, \end{aligned} \quad (6)$$

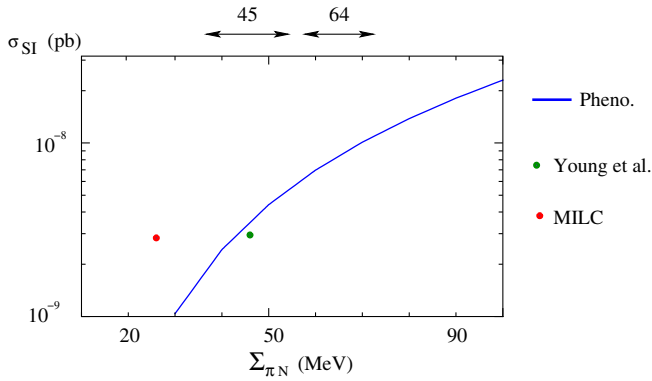


FIG. 3 (color online). Spin-independent elastic scattering cross section as function of the pion-nucleon sigma term $\Sigma_{\pi N}$ for a scalar dark matter respecting WMAP constraint: $m_s = 90$ GeV, $\lambda_{HS} = 0.2$, $m_h = 130$ GeV giving $\Omega_S h^2 = 0.102$. We also represent the central values of the cross section for the lattice simulations [42,43] labeled “MILC” and “Young,” respectively.

where $y = 2\langle N|\bar{s}s|N\rangle/\langle N|\bar{u}u + \bar{d}d|N\rangle = 1 - \sigma_0/\Sigma_{\pi N}$ represents the strange fraction in the nucleon. We show in Fig. 2 the dependence of f_q as function of $\Sigma_{\pi N}$. The two extreme values are obtained with the lower bound of $\Sigma_{\pi N}$ at 1σ extracted from [39] (37 MeV) and the higher bounds from [40] (71 MeV) which give for $(m_u, m_d, m_s, m_c, m_b, m_t, m_p) = (2.76, 5, 94.5, 1250, 4200, 171\,400, 938.3)$ [MeV]

$$\begin{aligned} f_u^{\min} &= 0.016, & f_u^{\max} &= 0.030, & f_d^{\min} &= 0.020, \\ f_d^{\max} &= 0.044, & f_s^{\min} &= 0.013, & f_s^{\max} &= 0.454. \end{aligned} \quad (7)$$

These limitations on the phenomenological estimation of the strange structure of the nucleon clearly open the way for lattice QCD to offer significant improvement. Using the Feynman-Hellman relation $f_q = (m_q/M_N)\partial M_N/\partial m_q$, different authors have extracted the light-quark and strangeness sigma terms (see [38] for a clear review). The last results obtained by the MILC Collaboration [42] and by the authors of (labeled “Young” from now on) [43] provide stringent new limits on the strange quark sigma terms. The modern lattice results for f_s agree that the size is substantially smaller than has been previously thought:

$$f_s^{\text{Young}} = 0.033 \pm 0.022, \quad f_s^{\text{MILC}} = 0.069 \pm 0.016. \quad (8)$$

These two results are marginally consistent, although there may be differences in how the derivative with respect to m_s is taken. Moreover, they tend to favor the smaller phenomenological evaluation of $\Sigma_{\pi N}$. In the following, we will consider the central values of f_q extracted from the Young *et al.* analysis and refer to it as the “lattice” one, $f_u = f_d = f_l = 0.050$, and $f_s = 0.033$, and the maximum and minimum values for f_q given by phenomenological Refs. [39,40] [Eq. (7)]. We adapted the code MICROMEAS [44] to the different values of f_q depending on the model we

used, and modified it to include the new couplings/spectrum/interactions induced by the singlet scalar extension of the SM.

As we can see in Fig. 3, these uncertainties have a strong impact on the direct detection cross section, up to 1 order of magnitude. We also plotted the value of σ_{SI} obtained by the two lattice groups that we took into consideration in our analysis, corresponding to the central values $(\Sigma_{\pi N}, \sigma_{\text{SI}}) = (26 \text{ MeV}, 2.84 \times 10^{-9} \text{ pb})$ [42] and $(47 \text{ MeV}, 2.95 \times 10^{-9} \text{ pb})$ [43]. We clearly see that the lattice results are much more in accordance with the lower bound on $\Sigma_{\pi N}$: $\sigma_{\text{SI}}^{\min}(\Sigma_{\pi N} = 37 \text{ MeV}) = 1.93 \times 10^{-9} \text{ pb}$, whereas $\sigma_{\text{SI}}^{\max}(\Sigma_{\pi N} = 71 \text{ MeV}) = 1.05 \times 10^{-8} \text{ pb}$. We compiled all the necessary values of f_i in the following table.

f_i	Lattice	Min	Max
f_u	0.050	0.016	0.030
f_d	0.050	0.020	0.044
f_s	0.033	0.012	0.454
$f_{c,t,b}$	0.867	0.952	0.472
$f = \Sigma f_i + 3 \times \frac{2}{27} f_H$	0.326	0.260	0.629

In the rest of the paper, we will always present our results with the evaluation of f_s given by the maximum and minimum allowed value for $\Sigma_{\pi N}$ and the lattice extraction of Young *et al.* (which gives a quite similar cross section to the one obtained by the MILC group as we concluded above).

We show in Fig. 4 the influence of the sigma terms in the region excluded/accessible by XENON100 for different Higgs masses. Clearly, for the lowest values of f_s , constraints on the parameter space become weaker because fewer points generate a cross section exceeding the direct detection bounds. We also represented the expectation of a XENON 1T experiment and showed that it would reach 80% of the WMAP allowed parameter space, but could not tell anything for a heavy Higgs boson $M_H \gtrsim 300$ GeV, which is complementary to the LHC searches: due to the specific decay modes of the Higgs boson, the LHC is more sensitive to a heavy Higgs than to a light one.

III. THE INVISIBLE HIGGS WIDTH: A XENON100/LHC COMPLEMENTARITY

Recently the XENON100 Collaboration released new data, the most stringent in the field of dark matter detection [2].² Moreover, recently the CRESST experiment released its analysis in the low mass region [48] and seems to converge with DAMA/LIBRA and CoGENT toward a possible light dark matter signal for a mass around 10 GeV [49]. In the meantime, if $m_s \lesssim M_H/2$ the invisible

²Keeping an eye on the results of COGENT collaborations [45], recent works showed either there exists a tension between XENON100 and COGENT [46], or not [47]. We thus safely decided not to discuss in detail the COGENT issue in our analysis.

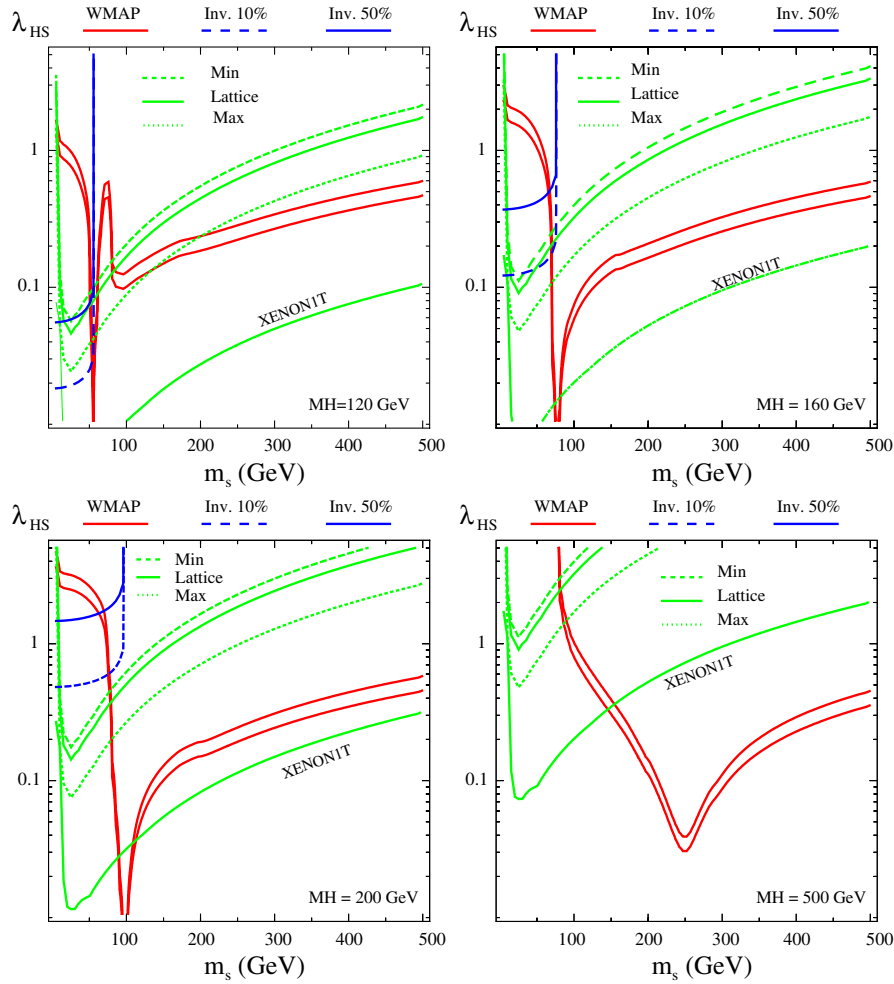


FIG. 4 (color online). Parameter space allowed in the plane (μ_S, λ_{HS}) for different Higgs masses (120, 160, 200, and 500 GeV) taking into account the last XENON100 data and the XENON 1T projection, with different values for the strange structure of the nucleon. We also show the invisible branching fraction of the Higgs boson width (10% and 50%, respectively). See the text for details.

width decay³ of the Higgs $H \rightarrow SS$ could perturbate the Higgs searches at the LHC based on the SM Higgs branching ratio [see Eq. (9) and [53] for a review on the SM Higgs width computation]. However, one can easily understand that there exists a tension between the direct detection measurement and the invisible branching ratio. Indeed, for decreasing mass of DM ($m_S \lesssim 100$ GeV), the spin-independent cross section increases. We show in Fig. 4 the regions in the $(m_S; \lambda_{HS})$ plane where the invisible branching fraction reaches 10% and 50% (dashed and full blue lines), for different values of the Higgs mass. As we noticed in the previous section, one needs a low value for λ_{HS} to respect the stringent XENON100 bounds. It is precisely in this regime ($m_S \lesssim M_H/2$) that the invisible width could interfere in the Higgs searches. However, the

low value of λ_{HS} restricted by XENON100 made this branching ratio very small. Quantitatively speaking, one needs to compare the invisible Higgs width ($H \rightarrow SS$)

$$\Gamma_H^{\text{inv}} = \frac{\lambda_{HS}^2 M_W^2}{32\pi g^2 M_H^2} \sqrt{M_H^2 - 4m_S^2} \quad (9)$$

with the spin-independent scattering cross section on the proton:

$$\sigma_{S-p}^{\text{SI}} = \frac{m_p^4 \lambda_{HS}^2 (\sum f_q)^2}{16\pi (m_p + m_S)^2 M_H^4}. \quad (10)$$

Combining Eqs. (9) and (10) one obtains

$$\frac{\Gamma_H^{\text{inv}}}{\sigma_{S-p}^{\text{SI}}} = \frac{(m_S + m_p)^2 M_H^2 M_W^2 \sqrt{M_H^2 - 4m_S^2}}{2g^2 f^2 m_p^4} \quad (11)$$

which reaches its maximum for $m_S - S^{\text{max}} = (-m_p + \sqrt{m_p^2 + 6M_H^2})/6 \approx 65.2$ GeV for $M_H = 160$ GeV, for instance. We can then compute the maximum value

³See the works in [50] for an earlier study of the invisible width of the Higgs. Moreover, during the revision of this study, several independent works confirming our results were published in [51,52].

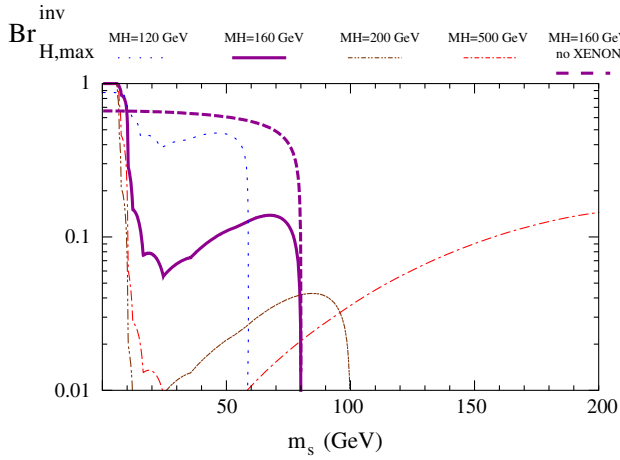


FIG. 5 (color online). Maximum Higgs invisible branching ratio as a function of the dark matter mass for different Higgs masses taking into account the last XENON100 constraint. We also show an example of invisible branching ratio for $M_H = 160$ GeV before taking into account the XENON100 constraint.

of the invisible width of the Higgs as a function of the scattering cross section on the proton:

$$\Gamma_{H,\max}^{\text{inv}} = \frac{(m_S^{\max} + m_p)^2 M_H^2 M_W^2 \sqrt{M_H^2 - 4(m_S^{\max})^2}}{2g^2 f^2 m_p^4} \sigma_{S-p}^{\text{SI}} \quad (12)$$

We show in Fig. 5 the value of the maximal branching ratio as a function of the dark matter mass for different values of M_H , taking into account the maximum value (m_S -dependent) of σ_{S-p}^{SI} allowed by the last data released by XENON100. We see that the XENON100 constraints impose a very low invisible Higgs branching ratio. To illustrate it, we also plotted a typical example of a branching ratio for $M_H = 160$ GeV *without* taking into account the XENON100 data (dashed magenta line). Whereas 80% of the Higgs could decay invisibly, after applying the XENON100 constraint on σ_{S-p}^{SI} its invisible branching fraction reaches only 10% *at its maximum* (corresponding to $m_S = m_S^{\max}$). Only for a very light Higgs ($M_H \lesssim 120$ GeV) Br_H^{inv} can reach 50%. The analysis was run with the value of the sigma terms of the nucleon given by the Young *et al.* analysis [43]. In fact, this choice is very conservative because if we took values of f_i corresponding to the maximum (unphysical) value of $\Sigma_{\pi N}$, we would obtain even a lower invisible width for the Higgs boson [Eq. (12)].

On top of that, when we include the WMAP constraint the allowed region shrinks and mainly branching fractions less than $\approx 10^{-1}$ still resist all the constraints. However, some points with a high invisible width still survive. They correspond to two distinct regions:

- (i) A region with a very light scalar ($m_S \lesssim 10$ GeV) still not yet excluded by the precision of XENON100 experiments due to its high threshold. This corresponds to a very large invisible branching ratio.

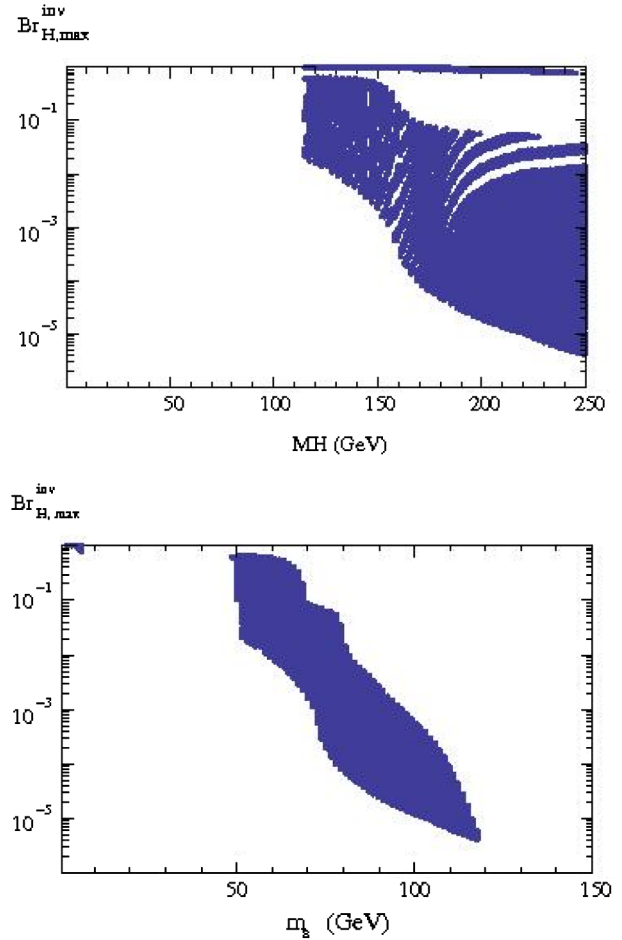


FIG. 6 (color online). Maximum Higgs invisible branching ratio as a function of the Higgs mass (top) and the dark matter mass (bottom) after a complete scan on λ_{HS} , m_s , and M_H taking into account the constraint on WMAP and applying the last XENON100 results. We clearly see that the points with a high invisible Higgs branching ratio are limited to a region with very low dark matter mass ($\lesssim 10$ GeV) and can reach $\sim 50\%$ for masses around 60 GeV as was noticed by [51]

- (ii) A region with $50 \text{ GeV} \lesssim m_s \lesssim 70 \text{ GeV}$ with a branching ratio which can reach 60% to 70% which is the region taken into consideration in [51].

We show the effects of combining WMAP and XENON100 data in Fig. 6. As one can see, except for these two particular regions, the majority of points respecting WMAP and XENON100 constraints give very low invisible width. As a conclusion, we can affirm that the Higgs searches at the LHC with scalar dark matter are not affected: the behavior of the Higgs is a standard model one, even including a singlet in the game. This is one of the strongest conclusions of this work, and the first level of complementarity between detection modes. It also means that we can use the standard Higgs limit searches of ATLAS and CMS and apply them in the model. They are only slightly affected by the presence of the scalar dark matter. However, in our numerical study, we obviously

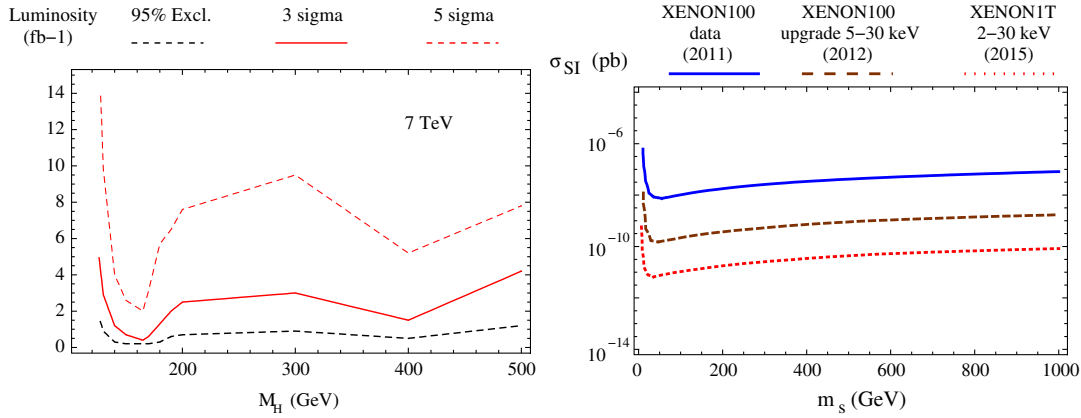


FIG. 7 (color online). Luminosity required to give exclusion (95% CL, dashed black), evidence (3σ full red), or discovery (5σ dashed red) sensitivity for a SM Higgs [57] with data at $\sqrt{s} = 7$ TeV (left); spin-independent WIMP-proton cross sections limit as a function of WIMP mass as measured by XENON100 [2] (full blue), and probed by different stages of the XENON program for 2012 (dashed brown) and 2015 (dotted red) [61].

took into consideration the invisible Higgs width to apply the CMS and ATLAS constraints.

Because of the last data released recently by the CRESST Collaboration [48] it is interesting to notice that some points in the parameter space around $m_s \approx 10$ GeV are not yet excluded by the latest XENON100 constraints as can be seen in the upper left corner of Fig. 6 (bottom). These points generate a Higgs completely invisible at the LHC. This corresponds to the region near $\text{Br}(H \rightarrow SS) \approx 100\%$ in Fig. 6 (top).

IV. THE HIGGS HUNTING: A LHC/XENON100 COMPLEMENTARITY

As we observed in Fig. 4, whereas the direct detection prospects are quite weak for a Higgs mass $M_H \gtrsim 300$ GeV, the XENON100 experiment will easily cover the region $M_H \lesssim 130$ GeV in the near future, which is precisely the region the most difficult to reach at the LHC. In the meantime, ATLAS [3] and CMS [4] with an integrated luminosity of 1 fb^{-1} have given at EPS [54] their first exclusion zone. CMS excludes the standard model Higgs in the 149–206 GeV and 300–440 GeV windows, while ATLAS excludes the 155–190 GeV and 295–450 GeV windows, whereas the combined result given at the Lepton Photon Conference [55] gives the two Higgs exclusion zones $145 < M_H < 288$ and $295 < M_H < 466$ at 95% of CL. The low mass exclusion is dominated by the search of the $H \rightarrow WW \rightarrow 2l2\nu$ final state, while the high mass one is dominated by $H \rightarrow ZZ$ after combining different Z decay channels.⁴ A summary and brief discussion of the analysis can be found in [56]. Combining all this analysis and being very conservative one can exclude the Higgs mass between 145 and 288 GeV and 295 and 466 GeV. CMS and ATLAS

⁴TEVATRON collaborations presented a combined analysis [6] and mainly agree on the results obtained by ATLAS and CMS.

could soon release a combined analysis closing the 288–295 windows. We show in Fig. 7 the luminosity required for a 95% exclusion 3σ and 5σ discovery potential for ATLAS [57]. We will use the results just released by ATLAS and CMS, and project the ATLAS 5σ projection for a luminosity of 10 fb^{-1} which will be the sensitivity reached by next year. We took the 5σ limit as we want to stay as conservative as possible; if we supposed that the Higgs (SM Higgs as we just pointed out in the previous section) can be excluded, all of the region 114–700 GeV could be excluded by the end of 2012, and thus the singlet extension of the SM.

In addition to the experimental constraints on the Higgs boson mass discussed previously, there are interesting constraints which can be derived from assumptions on the energy range in which the SM is valid before perturbation theory breaks down and new phenomena should appear. These include constraints from unitarity in scattering amplitudes, perturbativity of the Higgs self-coupling, stability of the electroweak vacuum, and fine-tuning. Whereas all the constraints bound roughly $M_H \lesssim 1$ TeV, the triviality bound which asks for perturbativity for the Higgs self-coupling λ_H [Eq. (1)], one obtains from simulation of gauge theory on lattice a rigorous bound $M_H \lesssim 640$ GeV. This limit is in remarkable agreement with the bound obtained by naively using the perturbation theory. Depending on the details of the cutoff scale, one can obtain an upper bound of 650 GeV [58] or 750 GeV [59]. We will use a rather secured value of 700 GeV (mean value of the two results) throughout the rest of the paper.⁵ The result of the combination of

⁵It was shown in [60] that one can lower a little bit the upper bound on the Higgs mass when the scalar singlet is included in the computation of the perturbativity limit, but this will affect the SM bound only for a cutoff scale $\Lambda_{\text{cutoff}} \gtrsim 10^7$ GeV. To be conservative, we will suppose through the study that $\Lambda_{\text{cutoff}} \gtrsim 1$ TeV.

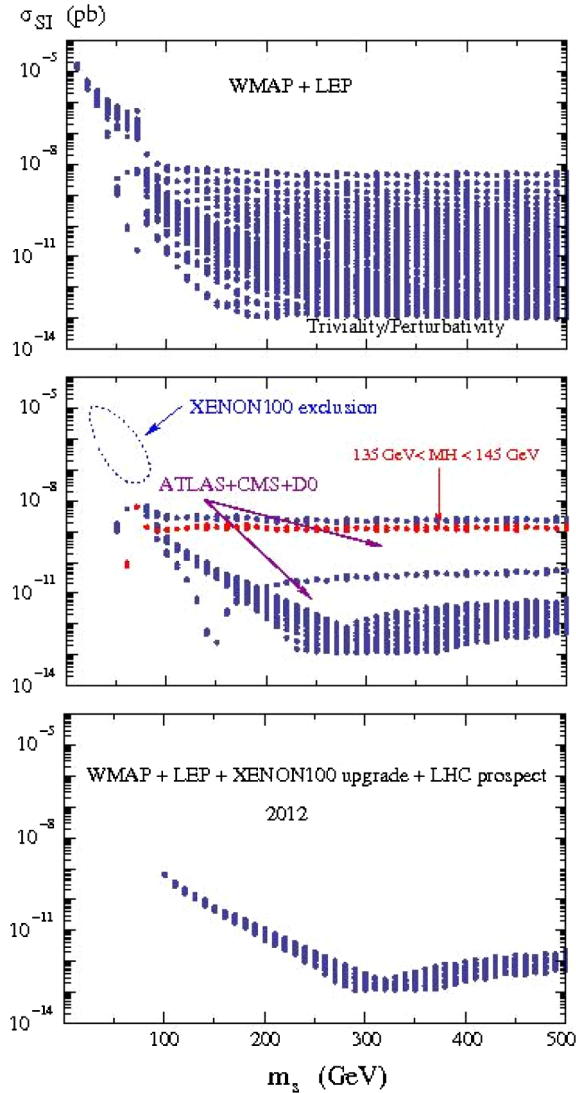


FIG. 8 (color online). Parameter space in the plane $(m_s; \sigma_{S-p}^{SI})$ still allowed after combining different constraints: WMAP, LEP, and triviality/perturbativity bound (top); XENON100, CMS, ATLAS, and D0 (middle); and prospect from ATLAS and XENON100 upgraded in the 5–30 keV range for 2012 (bottom). We also show in red (the lighter color in the middle panel) the region favored for a would-be Higgs boson mass $135 \text{ GeV} \lesssim M_H \lesssim 155 \text{ GeV}$.

the set of constraints we just discussed is presented in Fig. 8. We see that the influence of the LEP constraint on the Higgs mass (114 GeV) excludes a large part of the parameter space above $\sigma_{S-p}^{SI} \gtrsim 10^{-44} \text{ cm}^2$, whereas the triviality/perturbativity bound forbids $\sigma_{S-p}^{SI} \lesssim 10^{-49} \text{ cm}^2$ (Fig. 8, top). Meanwhile, the XENON100 data exclude the region of low DM mass and the high spin-independent cross section (Fig. 8, middle). Once one includes the CMS/ATLAS/D0 analysis, two large holes appear in the parameter space, which will be reduced in one hole by the end of the year with the CMS/ATLAS combined analysis. We plotted with red dots the

parameter space corresponding to a Higgs boson mass $135 < M_H < 155 \text{ GeV}$ (see the following section for more details).

We also show in Fig. 8 (bottom) the prediction expected for the next year (2012) taking into account the projected sensitivity of the XENON100 experiment [61] in an upgraded version of the detector where the photomultiplier tube array will be replaced by quartz photon intensifying detectors. Its sensitivity along with the projected 1 ton sensitivity is presented in Fig. 7 (right). We also took into account the projections for the ATLAS sensitivity to the standard model Higgs boson from the LHC running at center-of-mass energies of $\sqrt{s} = 7 \text{ TeV}$ [57]. This study extends the previous results of the collaboration by considering the luminosities required to reach 5σ discovery significance. The result of the analysis is presented in Fig. 7 (left), considering a 5σ Higgs discovery. We had to normalize this sensitivity $\mathcal{L} \rightarrow \mathcal{L}/(1 - \text{Br}_H^{\text{inv}})^2$ to take into account the invisible width of the Higgs.⁶ Once we take into consideration the whole set of predicted sensitivities, we observe (Fig. 8 bottom) that the main part of the parameter space should be easily covered by the end of next year. The only region which can escape the observation would be the one corresponding to the limit of perturbativity. We should then wait for the shutdown and upgraded version of the LHC to cover the *entire* parameter space of the model.

One of the key points of this analysis is based on the fact that the LHC collaborations will be able to reach a part of the parameter space which would never be reached by direct detection technologies because in the region of heavy Higgs ($M_H \gtrsim 300 \text{ GeV}$) one expects a very low direct detection rate ($\sigma_{S-p}^{SI} \lesssim 10^{-47} \text{ cm}^2$). In the meantime, the XENON100 experiment can exclude a part of the parameter space ($M_H \lesssim 118 \text{ GeV}$) which would necessitate a very high luminosity to be observed by ATLAS or CMS (see Fig. 7).

V. HIGGS SIGNAL?

Recently the ATLAS Collaboration quantified a 2.5σ excess for a Higgs boson mass 140–150 GeV. This is coherent when combined with the CMS and D0 result, corresponding to a mean value $M_H \approx 145 \text{ GeV}$. We plotted this “discovery” parameter space in Fig. 8. The points in red (the lighter color) respect WMAP and XENON100 constraints, in the range $135 \text{ GeV} < M_H < 145 \text{ GeV}$.⁷ From this region of parameter space, and including all the previous reliable constraints, one can deduce that $8 \times 10^{-46} \text{ cm}^2 \lesssim \sigma_{S-p}^{SI} \lesssim 2 \times 10^{-45} \text{ cm}^2$. Having a look

⁶Which is negligible in the large part of the parameter space allowed by XENON100.

⁷A similar analysis restricted to a region of parameter space where the invisible decay width of the Higgs reaches 40% has been developed in [51].

at Fig. 7, we can see that this region will unluckily not be reached by an upgraded version of the XENON100 experiment next year. In the meantime, a 1 ton extension would easily cover this region of the parameter space and would probe the singlet scalar dark matter paradigm, except in a very small region of the parameter space, where $m_S \lesssim 100$ GeV, which will be very difficult to observe with a XENON-like experiment.

However, one of the main issues is that the scattering cross section is independent of the DM mass. Indeed, if we combine Eqs. (A1) and (A3) we easily understand that for a given value of M_H and $\langle\sigma v\rangle$ (and so, to a relatively good approximation, of $\Omega_S h^2$) σ_{S-p}^{SI} is fixed independently of m_S once $m_S \gtrsim M_H$. This means that it will be difficult to determine the scalar mass even in projected direct detection experiments, like a 1T XENON-like.

It is also interesting to point out that the Higgs-portal construction is similar in several aspects to the Z' -portal model of dark matter [62]: as any Higgs searches restrict severely the parameter space of the model, any Z' searches at the LHC should be used in complementarity with direct detection searches to probe the entire parameter space allowed by WMAP. At the same time, the analysis should be done in a SUSY scenario where light Higgses are the main annihilation channel, leading to severe direct detection constraints [63].

Writing the conclusion of this work, we noticed that authors just looked at some consequences of recent Higgs searches at the LHC in the next-to-minimal supersymmetric standard model case [64] and extended scalar sectors [65].

VI. CONCLUSION AND PROSPECT

In this work, we studied the strong complementarity between the measurement of elastic scattering of dark matter on the nucleon and the Higgs searches at the LHC. We first studied in detail the influence of the new analysis of the strange quark content of the nucleon, especially from recent lattice results. We then showed that in a framework where the standard model is extended by a singlet scalar dark matter, combining the last

XENON100 experiment data with WMAP saves only the parameter space where the invisible decay branching ratio of the Higgs $\text{BR}^{\text{inv}}(H \rightarrow SS) \lesssim 10\%$, rendering the Higgs a standard model one, except in a small region with very light dark matter ($\lesssim 10$ GeV) not yet excluded by XENON100 or around 60 GeV where the ratio can reach 50% to 60%. We then applied the very recent searches of Higgs released by ATLAS, CMS, and D0 and excluded a huge part of the parameter space, which will be tested at 95% by the end of 2012. LHC collaborations will reach a region which could never be accessible by any kind of dark matter direct detection orientated experiments. Moreover, if one takes seriously the possibility of a hint around $M_H \simeq 145$ GeV, this would imply a scattering cross section of $\sigma_{S-p}^{\text{SI}} \simeq 10^{-45}$ cm², testable in the future upgraded version of XENON100. In any scenario, the next months of data/analysis will give precious answers to all these interrogations.

ACKNOWLEDGMENTS

The author wants to thank particularly J. B. Devivie, M. Tytgat, A. Falkowski, B. Zaldivar, and the Magic Monday Journal Club for (very) useful discussions. The work was supported by the French ANR TAPDMS ANR-09-JCJC-0146 and the Spanish MICINN's Consolider-Ingenio 2010 Programme under grant Multi-Dark CSD2009-00064.

APPENDIX: USEFUL FORMULAS

$$\langle\sigma_{f\bar{f}}v\rangle = \frac{\lambda_{HS}^2(m_S^2 - m_f^2)^{3/2}m_f^2}{16\pi m_S^3[(4m_S^2 - M_H^2)^2 + M_H^2\Gamma_H^2]} \quad (\text{A1})$$

$$\Gamma_H(H \rightarrow SS) = \frac{\lambda_{HS}^2 M_W^2}{32\pi g^2 M_H^2} \sqrt{M_H^2 - 4m_S^2} \quad (\text{A2})$$

$$\sigma_{S-p}^{\text{SI}} = \frac{m_p^4 \lambda_{HS}^2 (\sum_q f_q)^2}{16\pi(m_p + m_S)^2 M_H^4} \quad (\text{A3})$$

[1] D. N. Spergel *et al.* (WMAP Collaboration), *Astrophys. J. Suppl. Ser.* **170**, 377 (2007); E. Komatsu *et al.* (WMAP Collaboration), *Astrophys. J. Suppl. Ser.* **180**, 330 (2009).
 [2] E. Aprile *et al.* (XENON100 Collaboration), *Phys. Rev. D* **84**, 061101 (2011); *Phys. Rev. Lett.* **107**, 131302 (2011).
 [3] <https://atlas.web.cern.ch/Atlas/GROUPS/PHYSICS/CONFNOTES/ATLAS-CONF-2011-112/ATLAS-CONF-2011-112.pdf>.

[4] <http://cdsweb.cern.ch/record/1370076/files/HIG-11-011-pas.pdf>.
 [5] <http://www-d0.fnal.gov/Run2Physics/WWW/results/prelim/HIGGS/H112/H112.pdf>.
 [6] <http://www-d0.fnal.gov/Run2Physics/WWW/results/prelim/HIGGS/H97/H97.pdf>.
 [7] Y. Mambrini and B. Zaldivar, *J. Cosmol. Astropart. Phys.* **10** (2011) 023.
 [8] J. McDonald, *Phys. Rev. D* **50**, 3637 (1994).

- [9] J. McDonald, *Phys. Rev. Lett.* **88**, 091304 (2002).
- [10] M. Raidal and A. Strumia, *Phys. Rev. D* **84**, 077701 (2011).
- [11] C. P. Burgess, M. Pospelov, and T. ter Veldhuis, *Nucl. Phys.* **B619**, 709 (2001).
- [12] B. Patt and F. Wilczek, [arXiv:hep-ph/0605188](https://arxiv.org/abs/hep-ph/0605188).
- [13] K. A. Meissner and H. Nicolai, *Phys. Lett. B* **648**, 312 (2007).
- [14] H. Davoudiasl, R. Kitano, T. Li, and H. Murayama, *Phys. Lett. B* **609**, 117 (2005).
- [15] S.-h. Zhu, *Chin. Phys. Lett.* **24**, 381 (2007).
- [16] X.-G. He, T. Li, X.-Q. Li, J. Tandean, and H.-C. Tsai, *Phys. Rev. D* **79**, 023521 (2009); *Phys. Lett. B* **688**, 332 (2010); X.-G. He, S.-Y. Ho, J. Tandean, and H.-C. Tsai, *Phys. Rev. D* **82**, 035016 (2010).
- [17] S. Kanemura, S. Matsumoto, T. Nabeshima, and N. Okada, *Phys. Rev. D* **82**, 055026 (2010).
- [18] M. Aoki, S. Kanemura, and O. Seto, *Phys. Lett. B* **685**, 313 (2010).
- [19] W.-L. Guo and Y.-L. Wu, *J. High Energy Phys.* **10** (2010) 083.
- [20] V. Barger, Y. Gao, M. McCaskey, and G. Shaughnessy, *Phys. Rev. D* **82**, 095011 (2010).
- [21] J. R. Espinosa and M. Quiros, *Phys. Rev. D* **76**, 076004 (2007).
- [22] H. Sung Cheon, S. K. Kang, and C. S. Kim, *J. Cosmol. Astropart. Phys.* **05** (2008) 004.
- [23] V. Barger, P. Langacker, M. McCaskey, M. J. Ramsey-Musolf, and G. Shaughnessy, *Phys. Rev. D* **77**, 035005 (2008).
- [24] S. Andreas, T. Hambye, and M. H. G. Tytgat, *J. Cosmol. Astropart. Phys.* **10** (2008) 034.
- [25] S. Andreas, C. Arina, T. Hambye, F.-S. Ling, and M. H. G. Tytgat, *Phys. Rev. D* **82**, 043522 (2010).
- [26] M. H. G. Tytgat, *Proc. Sci. IDM2010* (2011) 126 [[arXiv:1012.0576](https://arxiv.org/abs/1012.0576)].
- [27] C. E. Yaguna, *J. Cosmol. Astropart. Phys.* **03** (2009) 003.
- [28] A. Goudelis, Y. Mambrini, and C. Yaguna, *J. Cosmol. Astropart. Phys.* **12** (2009) 008.
- [29] C. Arina and M. H. G. Tytgat, *J. Cosmol. Astropart. Phys.* **01** (2011) 011.
- [30] Y. Cai, X.-G. He, and B. Ren, *Phys. Rev. D* **83**, 083524 (2011).
- [31] A. Biswas and D. Majumdar, [arXiv:1102.3024](https://arxiv.org/abs/1102.3024).
- [32] M. Farina, M. Kadastik, D. Pappadopulo, J. Pata, M. Raidal, and A. Strumia, *Nucl. Phys.* **B853**, 607 (2011).
- [33] J. R. Ellis, K. A. Olive, and C. Savage, *Phys. Rev. D* **77**, 065026 (2008).
- [34] J. Giedt, A. W. Thomas, and R. D. Young, *Phys. Rev. Lett.* **103**, 201802 (2009).
- [35] X. Gao, Z. Kang, and T. Li, [arXiv:1107.3529](https://arxiv.org/abs/1107.3529).
- [36] M. A. Shifman, A. I. Vainshtein, and V. I. Zakharov, *Phys. Lett.* **78B**, 443 (1978).
- [37] A. I. Vainshtein, V. I. Zakharov, and M. A. Shifman, *Sov. Phys. Usp.* **23**, 429 (1980).
- [38] R. D. Young and A. W. Thomas, *Nucl. Phys.* **A844**, 266C (2010).
- [39] R. Koch, *Z. Phys. C* **15**, 161 (1982).
- [40] M. M. Pavan, I. I. Strakovsky, R. L. Workman, and R. A. Arndt, *PiN Newslett.* **16**, 110 (2002).
- [41] H.-Y. Cheng, *Phys. Lett. B* **219**, 347 (1989).
- [42] D. Toussaint *et al.* (MILC Collaboration), *Phys. Rev. Lett.* **103**, 122002 (2009).
- [43] R. D. Young and A. W. Thomas, *Phys. Rev. D* **81**, 014503 (2010).
- [44] G. Belanger, F. Boudjema, A. Pukhov, and A. Semenov, [arXiv:1005.4133](https://arxiv.org/abs/1005.4133); *Comput. Phys. Commun.* **180**, 747 (2009); **177**, 894 (2007).
- [45] C. E. Aalseth *et al.* (CoGeNT Collaboration), *Phys. Rev. Lett.* **106**, 131301 (2011).
- [46] T. Schwetz and J. Zupan, *J. Cosmol. Astropart. Phys.* **08** (2011) 008; M. T. Frandsen, F. Kahlhoefer, J. March-Russell, C. McCabe, M. McCullough, and K. Schmidt-Hoberg (private communication).
- [47] D. Hooper and C. Kelso, *Phys. Rev. D* **84**, 083001 (2011).
- [48] G. Angloher *et al.*, [arXiv:1109.0702](https://arxiv.org/abs/1109.0702).
- [49] C. Kelso, D. Hooper, and M. R. Buckley, [arXiv:1110.5338](https://arxiv.org/abs/1110.5338); J. Kopp, T. Schwetz, and J. Zupan, [arXiv:1110.2721](https://arxiv.org/abs/1110.2721).
- [50] M. C. Bento, O. Bertolami, and R. Rosenfeld, *Phys. Lett. B* **518**, 276 (2001); M. C. Bento, O. Bertolami, R. Rosenfeld, and L. Teodoro, *Phys. Rev. D* **62**, 041302 (2000).
- [51] M. Raidal and A. Strumia, [arXiv:1108.4903](https://arxiv.org/abs/1108.4903).
- [52] X.-G. He and J. Tandean, *Phys. Rev. D* **84**, 075018 (2011).
- [53] A. Djouadi, *Phys. Rep.* **457**, 1 (2008).
- [54] <http://eps-hep2011.eu/>.
- [55] <http://www.tifr.res.in/~lp11/>.
- [56] <http://blog.vixra.org/2011/07/22/big-day-for-higgs-boson/>; <http://resonaances.blogspot.com/>.
- [57] ATLAS, Report No. ATL-PHYS-PUB-2011-001, 2011.
- [58] M. Gockeler, H. A. Kastrup, T. Neuhaus, and F. Zimmermann, *Nucl. Phys.* **B404**, 517 (1993).
- [59] H. Neuberger, U. M. Heller, M. Klomfass, and P. M. Vranas, *Proceedings of the XXVI International Conference on High Energy Physics, Vol. II*, AIP Conf. Proc. No. 272 (AIP, New York, 1992), p. 1360.
- [60] M. Gonderinger, Y. Li, H. Patel, and M. J. Ramsey-Musolf, *J. High Energy Phys.* **01** (2010) 053.
- [61] E. Aprile and L. Baudis, *Proc. Sci.*, IDM2008 (2008) 018.
- [62] Y. Mambrini, *J. Cosmol. Astropart. Phys.* **07** (2011) 009; M. T. Frandsen, F. Kahlhoefer, S. Sarkar, and K. Schmidt-Hoberg, *J. High Energy Phys.* **09** (2011) 128; D. Feldman, B. Kors, and P. Nath, *Phys. Rev. D* **75**, 023503 (2007); Y. Mambrini, *J. Cosmol. Astropart. Phys.* **09** (2010) 022; **12** (2009) 005; K. Cheung and J. Song, *Phys. Rev. Lett.* **106**, 211803 (2011); E. Dudas, Y. Mambrini, S. Pokorski, and A. Romagnoni, *J. High Energy Phys.* **08** (2009) 014.
- [63] D. Das, A. Goudelis, and Y. Mambrini, *J. Cosmol. Astropart. Phys.* **12** (2010) 018; S. Bhattacharya, U. Chattopadhyay, D. Choudhury, D. Das, and B. Mukhopadhyaya, *Phys. Rev. D* **81**, 075009 (2010); A. Djouadi and Y. Mambrini, *J. High Energy Phys.* **12** (2006) 001.
- [64] U. Ellwanger, [arXiv:1108.0157](https://arxiv.org/abs/1108.0157).
- [65] X. G. He and G. Valencia, [arXiv:1108.0222](https://arxiv.org/abs/1108.0222).